Published in final edited form as:

Nature. 2010 October 14; 467(7317): 849–853. doi:10.1038/nature09409.

ETV1 is a lineage-specific survival factor in GIST and cooperates with KIT in oncogenesis

Ping Chi[1,2,10], **Yu Chen**[1,3,10], **Lei Zhang**[4], **Xingyi Guo**[5], **John Wongvipat**[3], **Tambudzai Shamu**[3], **Jonathan A. Fletcher**[6], **Scott Dewell**[7], **Robert G. Maki**[1], **Deyou Zheng**[5,8], **Cristina R. Antonescu**[4], **C. David Allis**[2,11], and **Charles L. Sawyers**[3,9,11]

[1] Department of Medicine, Memorial Sloan-Kettering Cancer Center, New York, New York, USA

[2] Laboratory of Chromatin Biology & Epigenetics, The Rockefeller University, New York, New York, USA

[3] Human Oncology and Pathogenesis Program, Memorial Sloan-Kettering Cancer Center, New York, New York, USA

[4] Department of Pathology, Memorial Sloan-Kettering Cancer Center, New York, New York, USA

[5] Department of Neurology, Albert Einstein College of Medicine, Bronx, New York, USA

[6] Department of Pathology, Brigham and Women's Hospital, Boston, Massachusetts, USA

[7] Genomics Resource Center, The Rockefeller University, New York, New York, USA

[8] Departments of Genetics and Neuroscience, Albert Einstein College of Medicine, Bronx, New York, USA

[9] Howard Hughes Medical Institute, Memorial Sloan-Kettering Cancer Center, New York, New York, USA

Abstract

Gastrointestinal stromal tumour (GIST) is the most common human sarcoma and is primarily defined by activating mutations in the *KIT* or *PDGFRA* receptor tyrosine kinases1,2. *KIT* is highly expressed in interstitial cells of Cajal (ICCs)—the presumed cell of origin for GIST—as well as in

Correspondence to: Charles L. Sawyers[3] and C. David Allis[2] Correspondence and requests for materials should be addressed to C.L.S. (sawyersc@mskcc.org) or C.D.A. (alliscd@rockefeller.edu).

[10]These authors contributed equally to this work

[11]These authors contributed equally to this work

Author contributions: PC, YC, CDA, and CLS designed the experiments. RGM and CRA provided critical advice regarding experimental design. PC and YC performed most of the experiments, including data mining, data analysis, tissue culture experiments, tissue processing, IF fluorescent microscopy, colony formation assays, and ChIP-Seq experiments. JW and TS performed xenograft some qRT-PCR experiments. LZ and CRA provided human tumour samples and performed FISH and IHC on them. SD performed the Solexa sequencing and genomic alignment, and XG and DZ analyzed ChIP-Seq data. JAF provided key experimental reagents. PC, YC and CLS wrote the manuscript. All authors discussed results and edited the manuscript.

Author Information

All microarray and ChIP-Seq data are available from the Gene Expression Omnibus database (http://www.ncbi.nlm.nih.gov/geo) under accession GSE22852.

The authors declare no competing financial interests.

hematopoietic stem cells, melanocytes, mast cells and germ cells2,3. Yet, families harbouring germline activating *KIT* mutations and mice with knock-in *Kit* mutations almost exclusively develop ICC hyperplasia and GIST4–7, suggesting that the cellular context is important for *KIT* to mediated oncogenesis. Here we show that the *ETS* family member *ETV1* is highly expressed in the subtypes of ICCs sensitive to oncogenic *KIT* mediated transformation8, and is required for their development. In addition, *ETV1* is universally highly expressed in GISTs and is required for growth of imatinib-sensitive and resistant GIST cell lines. Transcriptome profiling and global analyses of ETV1-binding sites suggest that ETV1 is a master regulator of an ICC-GIST-specific transcription network mainly through enhancer binding. The ETV1 transcriptional program is further regulated by activated KIT, which prolongs ETV1 protein stability and cooperates with ETV1 to promote tumourigenesis. We propose that GIST arises from ICCs with high levels of endogenous ETV1 expression that, when coupled with an activating KIT mutation, drives an oncogenic ETS transcription program. This differs from other *ETS*-dependent tumours such as prostate cancer, melanoma, and Ewing sarcoma where genomic translocation or amplification drives aberrant *ETS* expression9–11 and represents a novel mechanism of oncogenic transcription factor activation.

Reasoning that transcription factors are likely to play critical roles in defining the cellular context, we utilized three expression datasets12,13 to search for GIST specific genes that might provide new molecular insights. We identified an eleven-gene signature exclusively associated with GIST in all three datasets that included the *ETS* family transcription factor *ETV1* (Fig. 1a, Supplementary Table 1). Examination of individual tumour samples revealed that *ETV1* is highly expressed in all GISTs and at significantly higher levels than any other tumour type (Fig. 1b, Supplementary Fig. 1). *ETV1* was of immediate interest since *ETS* family transcription factors are well established oncogenes in Ewing sarcoma, melanoma, and prostate cancer9–11.

Next, we assessed mRNA and protein levels of ETV1 in GIST and other sarcomas in clinical samples, GIST cell lines (imatinib-resistant GIST48 and imatinib-sensitive GIST882), the U2OS osteosarcoma cell line, and the LNCaP prostate cancer cell line known to overexpress ETV1 due to translocation14 (Fig. 1c, d). ETV1 mRNA and protein were highly and exclusively expressed in all GISTs and GIST cell lines, and in LNCaP cells. As expected, *KIT* mRNA and protein were highly expressed in all GIST tumours and GIST cell lines, but not in other sarcomas or non-GIST cell lines, and phospho-KIT was only seen in GIST samples with activating *KIT* mutations. Four additional GIST samples amenable to immunohistochemical analysis all showed strong nuclear ETV1 staining whereas a leiomyosarcoma control sample did not (Supplementary Fig. 2). These data show that *ETV1* is universally highly expressed in all GISTs both at transcript and protein levels.

To explore the requirement of ETV1 in GIST pathogenesis, we performed RNAi experiments using two *ETV1*-specific hairpins validated for both protein and mRNA suppression (Supplementary Fig. 3a). Infection with either hairpin resulted in growth inhibition of both GIST cell lines, but did not affect the growth of U2OS cells. Consistent with the level of *ETV1* knockdown, ETV1sh2 was more growth suppressive than ETV1sh1 in both GIST cell lines (Fig. 1e). Cell cycle analysis showed that *ETV1* knockdown resulted

in both decreased cell cycle progression and increased apoptosis (Supplementary Fig. 3b). *ETV1* knockdown also impaired the tumourigenicity of GIST882 cells in SCID mouse xenografts, and those tumours that did grow had escaped *ETV1*suppression (Fig. 1f). Collectively, these observations indicate that ETV1 is required for GIST growth and survival.

Next, we addressed the mode of high *ETV1* expression in GIST. FISH on 4 GIST samples and 2 GIST cell lines showed no evidence of amplification or "breakaway" between the 3′ and 5′ ends of *ETV1* locus. qRT-PCR showed no evidence of differential exon expression, which is expected with *ETV1* translocation (Supplementary Fig. 4). Furthermore, no focal *ETV1* amplification was found in 40 GIST tumours and 6 GIST cell lines in a recent 250K SNP array study15. The fact that high levels of ETV1 expression are consistently observed in the absence of obvious genomic alterations raises the possibility that the ICCs that give rise to GIST may endogenously express *ETV1*.

The musculature of the GI tract is organized into two principal layers—the inner circular muscle (CM) layer beneath the mucosa (M) and the outer longitudinal muscle (LM) layer16. In the large intestine, myenteric ICCs (ICC-MY) form a network between the CM and LM layers surrounding the neuronal myenteric plexus, intramuscular ICCs (ICC-IM) are singly dispersed in the CM, and submucosal ICCs (ICC-SMP) form network surrounding the submucosal plexus (Fig. 2a). In the small intestine, ICC-IMs and ICC-SMPs are absent and ICC-DMPs form a network around the deep muscular plexus in the CM close to the mucosa (Supplementary Fig. 5a). All four ICC subtypes are identified by positive membrane expression of Kit16 (Fig. 2b and Supplementary Fig. 5b). In the large intestine, ICC-MYs and ICC-IMs but not ICC-SMPs stain with nuclear Etv1 (Fig. 2b). In the small intestine, ICC-MYs but not ICC-DMPs stain with nuclear Etv1 (Supplementary Fig. 5b). This finding is further supported by our analysis of a published ICC expression dataset from mouse small intestine17 showing that *Etv1* is only highly expressed in ICC-MYs (Supplementary Fig. 5c). Notably, in the *Kit*Δ^{558} mutant mice only ICC-MY and ICC-IM develop hyperplasia while ICC-SMP and ICC-DMP do not8. These data suggest that ETV1 is a lineage-specific transcription factor for the ICCs that give rise to GIST.

We therefore asked if Etv1 is required for the normal development of ICCs by examining the GI tracts of *Etv1*$^{-/-}$ mice18. Cross section and reconstructed whole-mount images from *Etv1*$^{-/-}$ mice showed significant loss of Kit-positive ICC-IMs and ICC-MYs in the large intestine (Fig. 2c–d, Supplementary Fig. 9, Supplementary Movies 1–2), small intestine, stomach, and cecum (Supplementary Figs. 6–9, Supplementary Movies 3–8). In contrast, ICC-DMPs and ICC-SMPs in the small and large intestine respectively were preserved, consistent with absent Etv1 expression in these ICC subtypes. These results were confirmed with a second ICC marker Ano119 (Supplementary Fig. 10). Immunostaining with the neuronal marker PGP9.5 confirmed the integrity of the myenteric plexus in *Etv1*$^{-/-}$ mice (Fig. 2c, Supplemental Figs. 6–8, 11). Collectively, these data indicate that Etv1 is selectively required for development of ICC-MY and ICC-IM and, by implication, a lineage-specific survival factor for the ICC-GIST lineage.

To identify ETV1 target genes in GIST, we analyzed the effect of shRNA-mediated *ETV1* suppression on the transcriptomes of GIST48 and GIST882 cells. The overlap of genes perturbed by both *ETV1*-specific hairpins and across both cell lines was highly statistically significant, suggesting that ETV1 regulates a core set of genes in GIST (Supplementary Fig. 12). To minimize cell line-specific and off-target effects, we generated a ranked gene list based on the average change in gene expression induced by the two *ETV1*-specific hairpins in both GIST cell lines (Fig. 3a, b). We independently confirmed downregulation of 5 of these genes using real-time RT-PCR (Supplementary Fig. 13). Among the 48 genes suppressed >1.7-fold by *ETV1* knockdown, 32 were expressed at higher levels in human GIST samples relative to other tumour types in the ExpO expression dataset (Fig. 3b). We performed gene set enrichment analysis (GSEA)20 of the "shETV1" ranked list using >3,000 gene sets in the Molecular Signature Database along with 5 custom gene sets defined by GIST-signature genes from the Segal, Nielsen, and ExpO datasets and by ICC-MY- and ICC-DMP-signature genes (Supplementary Table 1). All three GIST sets along with the ICC-MY set were among the most negatively enriched gene sets while the ICC-DMP set was not (Fig. 3c, Supplementary Fig. 14, and Supplementary Table 2). These data suggest that *ETV1* is a master regulator of a transcriptional program conserved in ICC-IM/MYs and GISTs.

To define the direct transcriptional targets of ETV1 in GIST, we performed genome-wide analyses of ETV1-binding sites using ChIP-Seq in GIST48 cells. We identified 14,741 ETV1-binding sites (ETV1 peaks) which are enriched in promoter regions (Fig. 3d). Motif analysis of the peaks identified the ETS core consensus motif, GGAA, in ~90% of peaks (Fig. 3f). Integrative analyses of the ETV1 ChIP-Seq data with the transcriptomes from shRNA-mediated *ETV1* suppression in GIST cells showed that 38 of the top 48 shETV1 downregulated genes contain ETV1 peaks (Fig. 3b, e, Supplementary Fig. 15). Analysis of genes with 1.4-fold change by shETV1 knockdown revealed that both shETV1 upregulated and shETV1 downregulated genes are enriched for ETV1 peaks. Furthermore, enhancer binding and in particular enhancer and promoter binding is highly predicative of transcriptional activation by ETV1 (Fig. 3h). Since enhancers are in general cell-lineage specific21,22, our data suggest that these ICC-GIST-lineage specific genes are likely directly regulated by ETV1 binding to their enhancer regulatory elements.

The dual requirement of *KIT* and *ETV1* in normal ICC development and GIST survival raise the possibility that KIT and ETV1 cooperate in GIST oncogenesis. Inhibition of KIT signalling by imatinib in imatinib-sensitive GIST882 cells resulted in rapid loss of ETV1 protein, without significant effect on *ETV1* mRNA levels (Fig. 4a, b, Supplementary Fig. 16). Similar results were observed with the MEK inhibitor PD325901. This loss of ETV1 protein was faster than the natural degradation rate, as revealed by cyclohexamide experiments to inhibit protein synthesis, and was rescued from proteosomal degradation by MG132 (Fig. 4b). Therefore, KIT-MEK signalling stabilizes ETV1 protein. Consistent with this KIT-MEK-ETV1 signalling pathway model, the overlap between genes transcriptionally altered by imatinib treatment (KIT-regulated) and by ETV1 knockdown in GIST882 cells is highly significant (Fig. 4c). Furthermore, these ETV1 transcriptional targets preferentially

contain ETV1 enhancer peaks (Fig. 4d), indicating that KIT signalling influences the ETV1 transcriptional output of the tissue and lineage-specific genes in GIST.

Having established a signalling pathway from KIT to ETV1, we explored their potential cooperativity in tumourigenesis by expressing *ETV1*, wild-type *KIT*, *KIT* harbouring a common GIST mutation (*KITΔ560*) and control vectors in combination in NIH3T3 cells. KIT-dependent stabilization of ETV1 protein was recapitulated in this system (Fig. 4e). In anchorage independent colony formation assays, ETV1 significantly increased the number and size of colonies in KITΔ560 expressing cells but was insufficient to confer anchorage-independent growth on its own (Supplementary Fig. 17). Furthermore, KITΔ560 and ETV1 strongly cooperated in conferring tumourigenic growth in SCID mice (Fig. 4f, g).

Taken together, these findings establish an oncogenic role for ETV1 in GIST that differs from classical models of *ETS*-driven malignancies where structural alterations (e.g., *TMPRSS2-ETV1* translocation in prostate cancer, *ETV1* amplification in melanoma) lead to aberrant expression and promote tumourigenesis9,11. Rather, ETV1 expression in GIST is inherited from ICC-MY/IM cells, where ETV1 is also a survival factor. We further established that KIT activity, through MEK, stabilizes ETV1, providing a mechanism for KIT-ETV1 cooperativity (Fig. 4h). These observations provide an explanation for why patients and mice with germline activating *KIT* mutations develop neoplasia in only the ICC-MY/IM lineage. While the mechanism of *ETV1*-mediated oncogenesis in GIST differs from other *ETS*-driven cancers, we anticipate that the *ETV1*-dependent transcriptional program defined here may serve as a valuable resource for further understanding of other *ETV1*- and other *ETS*-driven transcriptional programs in various cellular contexts such as prostate cancer.

The fact that ETV1 is universally highly expressed in all GISTs makes it immediately useful as a candidate diagnostic biomarker, since the current standard of KIT immunoreactivity is negative in about 5% of all GISTs23. While transcription factors has classically been considered “undruggable”, reports of successful inhibition of the NOTCH transcription factor complex and AR activity by blocking coactivator binding have challenged this paradigm24,25. Due to established requirements of ETV1 in subsets of prostate cancer and melanoma, efforts to find ETV1 inhibitors are underway and may yield novel therapeutic agents for imatinib-resistant GIST.

Methods Summary

Expression data mining, microarray analysis and ChIP-Seq

All mined datasets were downloaded Gene Expression Omnibus (GSE2109, GSE7809, GSE2719, GSE3443, GSE8167, GSE17743) and were analyzed by Oncomine™ or using Genespring 10. GIST-signature genes from three datasets containing both GIST and non-GIST malignancies met the following two criteria: 1) $q<0.05$, and 2) a Z-score expression difference >1.5 between GIST and non-GIST tumours. Expression profiling of GIST cell lines with different shRNA conditions was performed in duplicate on Illumina Human HT-12 array. GSEA was performed using MSigDB C2, MSigDB C4, and the GIST and ICC signature gene sets. For ChIP-Seq, sheared chromatin enriched by ETV1 IP was sequenced

on Solexa Genome Analyzer, aligned using ELAND alignment software. Peaks were identified by MACS using input DNA as control using a FDR <1%.

Materials

GIST48 and GIST882 cells were established in the Fletcher laboratory (DFCI). All other cells were obtained from ATCC. *Etv1*$^{-/-}$ mice, with targeted deletion of the ETS domain, was obtained from the Jessell laboratory (Columbia) and CB17-SCID mice was from Taconic. Antibody sources are: ETV1, ANO1, PGP9.5 (Abcam), KIT for WB, P-Tyr703-KIT (Cell Signaling), P-Tyr204-ERK, GAPDH (Santa Cruz), and anti-mouse Kit for IF (clone ACK2, E-Biosciences).

Supplementary Material

Refer to Web version on PubMed Central for supplementary material.

Acknowledgments

This work is supported in part by the NCI (K08CA140946, YC), (5F32CA130372, PC), (CA47179, CRA, RGM), (CA148260, RGM), US NIMH (R21MH087840, DZ), NCI-ASCO Cancer Foundation Clinical Investigator Team Leadership Supplemental Award (RGM), ASCO YIA (PC), Doris Duke (CLS), Charles H Revson (YC), the Charles A. Dana (YC) Foundations, ACS MRSG CCE-106841 (CRA), P01CA47179 (CRA, RGM), Life Raft Group (CRA), GIST Cancer Research Fund (CRA), Shuman Family Fund for GIST Research (CRA, RGM), Cycle for Survival (RGM) and Startup Funds from Albert Einstein College of Medicine (DZ). We thank International Genomics Consortium (IGC) for generating ExpO data. We thank G. Wang, P. Iaquinta, and H. Hieronymus for discussions, and especially T. M. Jessell and J. N. Betley for providing and breeding *Etv1*$^{-/-}$ mice.

References

1. Heinrich MC, et al. PDGFRA activating mutations in gastrointestinal stromal tumors. Science. 2003; 299:708–710. [pii]. 10.1126/science.1079666 [PubMed: 12522257]
2. Hirota S, et al. Gain-of-function mutations of c-kit in human gastrointestinal stromal tumors. Science. 1998; 279:577–580. [PubMed: 9438854]
3. Kindblom LG, Remotti HE, Aldenborg F, Meis-Kindblom JM. Gastrointestinal pacemaker cell tumor (GIPACT): gastrointestinal stromal tumors show phenotypic characteristics of the interstitial cells of Cajal. Am J Pathol. 1998; 152:1259–1269. [PubMed: 9588894]
4. Antonescu CR. Gastrointestinal stromal tumor (GIST) pathogenesis, familial GIST, and animal models. Semin Diagn Pathol. 2006; 23:63–69. [PubMed: 17193819]
5. Nakai N, et al. A mouse model of a human multiple GIST family with KIT-Asp820Tyr mutation generated by a knock-in strategy. J Pathol. 2008; 214:302–311.10.1002/path.2296 [PubMed: 18098338]
6. Rubin BP, et al. A knock-in mouse model of gastrointestinal stromal tumor harboring kit K641E. Cancer Res. 2005; 65:6631–6639. 65/15/6631 [pii]. 10.1158/0008-5472.CAN-05-0891 [PubMed: 16061643]
7. Sommer G, et al. Gastrointestinal stromal tumors in a mouse model by targeted mutation of the Kit receptor tyrosine kinase. Proc Natl Acad Sci U S A. 2003; 100:6706–6711. [pii]. 10.1073/pnas.1037763100 [PubMed: 12754375]
8. Kwon JG, et al. Changes in the structure and function of ICC networks in ICC hyperplasia and gastrointestinal stromal tumors. Gastroenterology. 2009; 136:630–639. S0016-5085(08)01866-0 [pii]. 10.1053/j.gastro.2008.10.031 [PubMed: 19032955]
9. Tomlins SA, et al. Recurrent fusion of TMPRSS2 and ETS transcription factor genes in prostate cancer. Science. 2005; 310:644–648. 310/5748/644 [pii]. 10.1126/science.1117679 [PubMed: 16254181]

10. Mertens F, et al. Translocation-related sarcomas. Semin Oncol. 2009; 36:312–323. S0093-7754(09)00104-3 [pii]. 10.1053/j.seminoncol.2009.06.004 [PubMed: 19664492]
11. Jane-Valbuena J, et al. An oncogenic role for ETV1 in melanoma. Cancer Res. 2010; 70:2075–2084. 0008-5472.CAN-09-3092 [pii]. 10.1158/0008-5472.CAN-09-3092 [PubMed: 20160028]
12. Nielsen TO, et al. Molecular characterisation of soft tissue tumours: a gene expression study. Lancet. 2002; 359:1301–1307. S0140-6736(02)08270-3 [pii]. 10.1016/S0140-6736(02)08270-3 [PubMed: 11965276]
13. Segal NH, et al. Classification and subtype prediction of adult soft tissue sarcoma by functional genomics. Am J Pathol. 2003; 163:691–700. [PubMed: 12875988]
14. Tomlins SA, et al. Distinct classes of chromosomal rearrangements create oncogenic ETS gene fusions in prostate cancer. Nature. 2007; 448:595–599. [PubMed: 17671502]
15. Beroukhim R, et al. The landscape of somatic copy-number alteration across human cancers. Nature. 2010; 463:899–905. nature08822 [pii]. 10.1038/nature08822 [PubMed: 20164920]
16. Ward SM, Sanders KM. Physiology and pathophysiology of the interstitial cell of Cajal: from bench to bedside. I. Functional development and plasticity of interstitial cells of Cajal networks. Am J Physiol Gastrointest Liver Physiol. 2001; 281:G602–611. [PubMed: 11518672]
17. Chen H, et al. Differential gene expression in functional classes of interstitial cells of Cajal in murine small intestine. Physiol Genomics. 2007; 31:492–509. 00113.2007 [pii]. 10.1152/physiolgenomics.00113.2007 [PubMed: 17895395]
18. Arber S, Ladle DR, Lin JH, Frank E, Jessell TM. ETS gene Er81 controls the formation of functional connections between group Ia sensory afferents and motor neurons. Cell. 2000; 101:485–498. S0092-8674(00)80859-4 [pii]. [PubMed: 10850491]
19. Gomez-Pinilla PJ, et al. Ano1 is a selective marker of interstitial cells of Cajal in the human and mouse gastrointestinal tract. Am J Physiol Gastrointest Liver Physiol. 2009; 296:G1370–1381. 00074.2009 [pii]. 10.1152/ajpgi.00074.2009 [PubMed: 19372102]
20. Subramanian A, et al. Gene set enrichment analysis: a knowledge-based approach for interpreting genome-wide expression profiles. Proc Natl Acad Sci U S A. 2005; 102:15545–15550. 0506580102 [pii]. 10.1073/pnas.0506580102 [PubMed: 16199517]
21. Heintzman ND, et al. Histone modifications at human enhancers reflect global cell-type-specific gene expression. Nature. 2009; 459:108–112. nature07829 [pii]. 10.1038/nature07829 [PubMed: 19295514]
22. Visel A, et al. ChIP-seq accurately predicts tissue-specific activity of enhancers. Nature. 2009; 457:854–858. nature07730 [pii]. 10.1038/nature07730 [PubMed: 19212405]
23. Miettinen M, Lasota J. Gastrointestinal stromal tumors: review on morphology, molecular pathology, prognosis, and differential diagnosis. Arch Pathol Lab Med. 2006; 130:1466–1478. RA-5-1116 [pii]. [PubMed: 17090188]
24. Andersen RJ, et al. Regression of castrate-recurrent prostate cancer by a small-molecule inhibitor of the amino-terminus domain of the androgen receptor. Cancer Cell. 2010; 17:535–546. S1535-6108(10)00200-X [pii]. 10.1016/j.ccr.2010.04.027 [PubMed: 20541699]
25. Moellering RE, et al. Direct inhibition of the NOTCH transcription factor complex. Nature. 2009; 462:182–188. nature08543 [pii]. 10.1038/nature08543 [PubMed: 19907488]

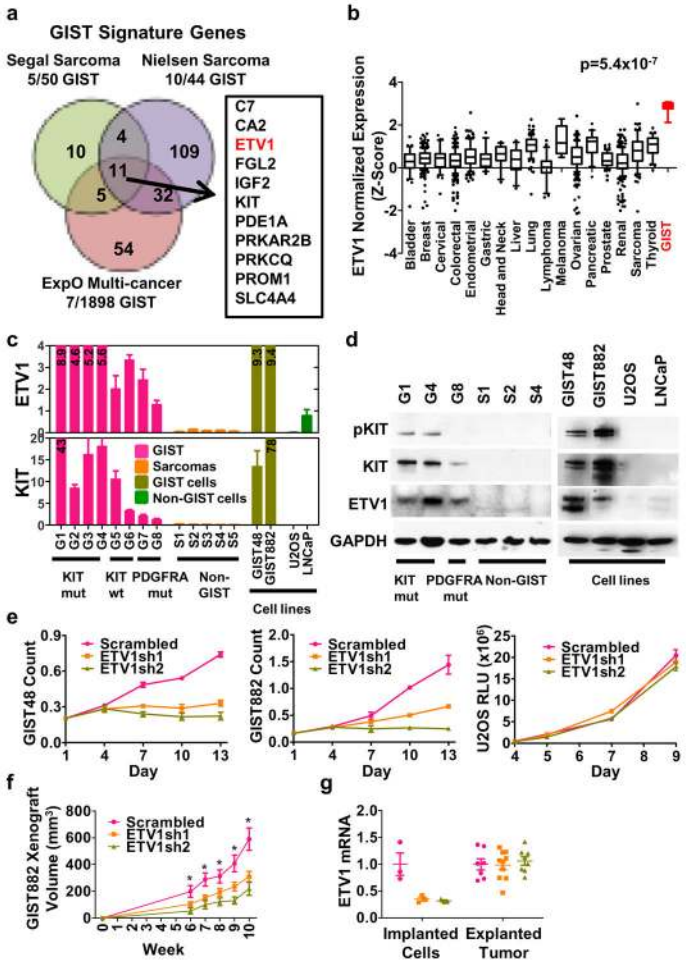

Figure 1. ETV1 is universally highly expressed and required for tumour growth and survival in GIST

a, Venn diagram of GIST-signature genes from three datasets. **b**, Expression of *ETV1* in multiple tumour types from the ExpO dataset. Box, 25–75 percentile; error bar, 10–90 percentile; dots, outliers. **c**, *ETV1* and *KIT* mRNA levels by qRT-PCR of GIST and non-GIST samples, whose details are described in Full Methods. Mean±SD, n=3. **d**, Immunoblotting of selected tumour tissues and cell lines from **c. e**, Growth curves of GIST and U2OS cells after shRNA-mediated *ETV1* suppression compared to control. Mean±SEM, n=3. **f**, Tumour volume over time in SCID mice implanted with GIST882 cells after shRNA-mediated *ETV1* suppression compared to scrambled shRNA controls. Mean±SEM, * $p<0.05$; n=7, 10, 8 for scrambled, ETV1sh1, and ETV1sh2 respectively. **g**, *ETV1* mRNA levels of preimplanted GIST882 cells and explanted xenografts at week 10. Mean±SD.

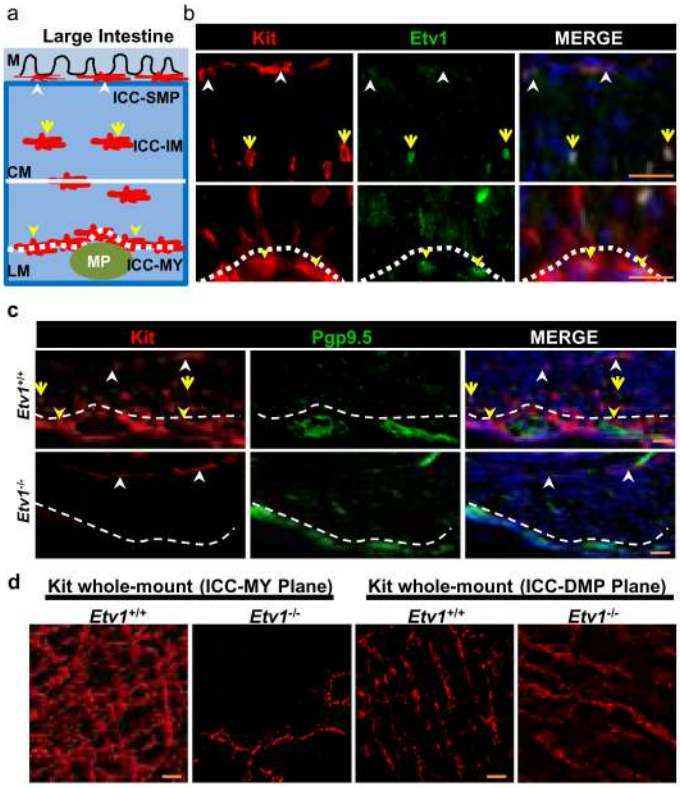

Figure 2. Etv1 is expressed in the subtypes of ICCs susceptible to oncogenesis and is required for their development

a, Schematic showing localization of ICC-MY (yellow arrowheads), ICC-IM (yellow arrows) and ICC-SMP (white arrowheads) in the large intestine. M: mucosa, CM: circular muscle, LM: longitudinal muscle. All three ICC subtypes express Kit (red).**b**, Co-immunofluorescence (divided into two microscopy fields) of Kit (red), Etv1 (green) and DAPI (blue) of the large intestine of wild-type mice. **c**, Co-immunofluorescence of Kit (red), Pgp9.5 (green), and DAPI (blue) of the large intestine of *Etv1*$^{+/+}$ and *Etv1*$^{-/-}$ mice. **d,** Representative deconvoluted whole-mount Kit-immunofluorescence images of the large intestine of *Etv1*$^{+/+}$ and *Etv1*$^{-/-}$ mice. A single microscopy field focused to the ICC-MY and ICC-SMP planes are shown. The entire Z-stacks are shown in Supplemental Movies 1, 2. Scale bar, 20 μm.

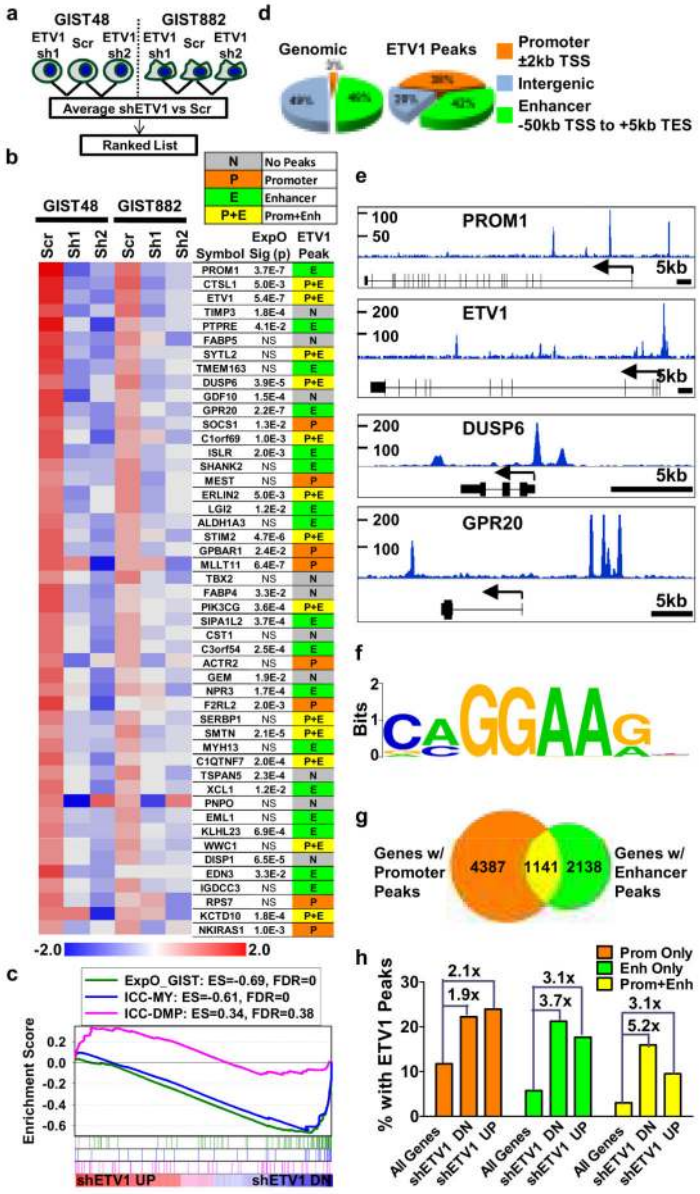

Figure 3. ETV1 regulates GIST-signature genes predominantly through enhancer binding

a, Ranked list of ETV1 regulated genes was generated based on the average fold-change by the two *ETV1* hairpins in two cell lines. **b**, Heatmap of expression of the 48 genes with average downregulation >1.7-fold. For each gene, table shows p-value of GIST vs. other tumour types from the ExpO dataset, calculated by Oncomine™ (NS: p>0.05), and the presence of ETV1 binding sites from ChIP-Seq analysis. **c,** GSEA plots of the shETV1 ranked list using three gene sets: GIST signature genes from ExpO dataset, ICC-MY and ICC-DMP signature genes in mouse small intestine. ES, enrichment score; FDR, false discovery rate. **d**, Pie charts of genomic structure and distribution of ETV1 ChIP-Seq peaks. TSS, transcription start site; TES, transcription end site. **e**, Representative ChIP-Seq reads in top ETV1 target genes. **f**, The consensus sequence motif identified in the ETV1 binding sites by the MEME program. **g**, Pie chart of genes with ETV1 binding sites divided into promoter

only, enhancer only and both. **h**, Plot of percent of all genes, genes averagely downregulated 1.4-fold by shETV1 (n=410), and genes averagely upregulated 1.4-fold by shETV1 (n=380) with promoter only, enhancer only and both promoter and enhancer ETV1 binding. Fold enrichment over all genes is shown above the plots.

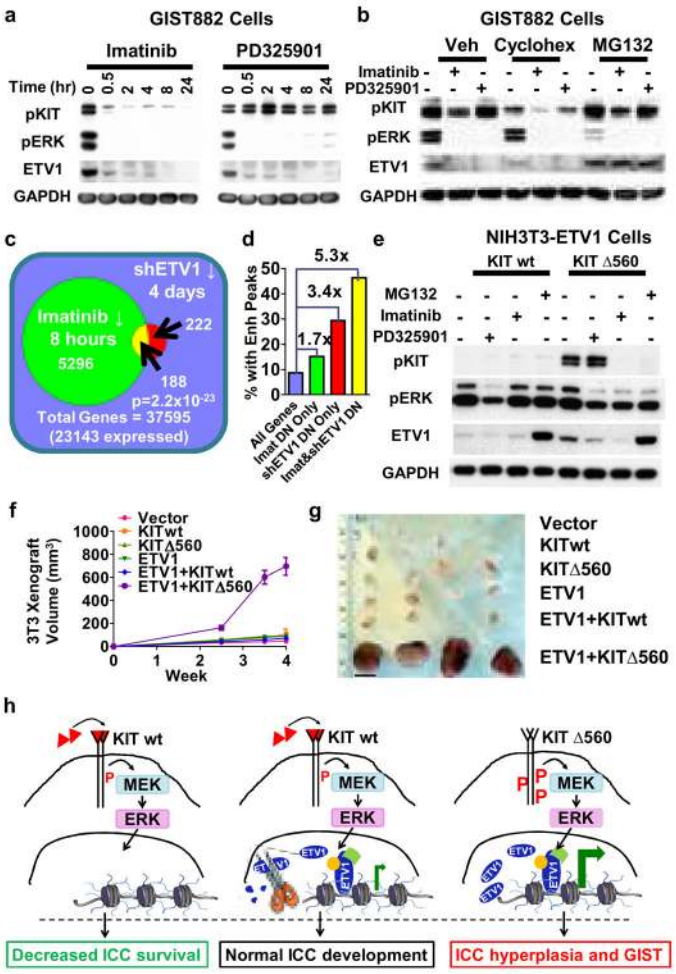

Figure 4. KIT signalling synergizes with ETV1 in GIST tumourigenesis by stabilization of ETV1 protein

a, Immunoblots of GIST882 cells treated with the imatinib (1 μM) and PD325901 (100 nM) for the indicated time points. **b,** Immunoblots of GIST882 cells treated for 2 hours with imatinib or PD325901 in combination with cyclohexamide (10 μg/ml) or MG132 (10 μM). **c**, Venn diagram of genes downregulated by 1.4-fold by shETV1 and by imatinib in GIST882 cells. P-value: Fisher's exact test based on number of expressed genes. **d**, Percent of all genes, imatinib-downregulated genes, shETV1-downregulated genes, and overlapping genes with ETV1 enhancer peaks. **e,** Immunoblot of NIH3T3 cells expressing *ETV1* and either *KITwt* or *KITΔ560* two hours after treatment with PD325901, imatinib, or MG132. **f,** Growth of xenografts of engineered NIH3T3 cells stabilizing the indicated genes (n=12, Mean ±SEM). **g**, Photograph of 4 representative explanted xenografts at 4 weeks after implanting. Scale bar 1 cm. **h**, Model of the role of ETV1 in ICC maintenance and GIST oncogenesis. Normal level of KIT activation by KIT ligand (red triangle) stabilizes ETV1 transcription factor through the MAPK pathway, and results in physiological ETV1 transcriptional output critical for ICC development (middle). In the absence of ETV1, there is decreased ICC development, which phenocopies genetic loss of KIT signalling (left). Activating mutation of *KIT* (e.g. *KITΔ560*) leads to constitutive activation of the KIT-

MAPK signalling pathway, increased stabilization and augmented ETV1 transcriptional output that promotes tumourigenesis (right).